

Characterization of Biochar Derived from Durian Shells by Pyrolysis Process

Sutatip Thonglem^{1*} and Pratthana Intawin²

Received: March 20, 2020; Revised: April 26, 2020; Accepted: April 28, 2020

Abstract

The objective of this research was to study the properties of durian shells biochars prepared by the pyrolysis process. The durian shells were contained in a closed chamber and heated in an electric furnace at different temperatures which varied from 500 °C to 900 °C for 10 hours. After heating, durian shells turned into black color. Density and porosity, surface morphology, elemental compositions, and crystalline phases of biochars were investigated by Archimedes immersion technique, scanning electron microscope (SEM), Energy dispersive x-ray spectrometry (EDX) and X-ray diffractometer (XRD), respectively. An increase in pyrolysis temperature led to yield reduction and an increase in the bulk density of biochars. SEM analysis showed the distribution of pore on all biochars fractures with similar apparent porosity values of more than 70%. The main elements in all biochars contained carbon (C) and oxygen (O), which were studied by EDX analysis. XRD results showed phase formation of carbon in biochar, which could form both amorphous and semi-crystalline phases. While oxygen could be composed in other elements in biomass through many forms of mineralogical compositions as CaCO₃ (Calcite), KHCO₃ (kalicinite), and Ca₃(PO₄)₂. Moreover, the alkali lignin phase appears in biochar at 500 °C and 600 °C conditions because of a highly cross-linked structure of the lignin. The CaCO₃ and Ca₃(PO₄)₂ phases could decompose at low pyrolysis temperature, but KHCO₃ phase formed at high temperatures hence the thermal stability of the KHCO₃ phase was higher than CaCO₃ and Ca₃(PO₄)₂ phases.

Keywords: Durian Shells; Biochar; Carbon; Pyrolysis Process

¹ Faculty of Science and Technology, Phranakorn Rajabhat University, Bangkok

² Faculty of Science and Technology, Rajamangala University of Technology Thanyaburi, Pathum Thani

* Corresponding Author E - mail Address: sutatip.t@pnru.ac.th

Introduction

Currently, severe problems throughout the world are energy crisis, environmental pollution, and global warming. The utilization of clean energy sources and the development of renewable energy sources can be considered as good choices for alleviating these problems. The synthesis of energy storage materials used in supercapacitors and Li-ion batteries is essential and challenging [1]. Carbon-based materials fabricated to electrodes show to achieve high electrical conductivity, chemical stability, and power density in superconductors. The advanced carbon materials such as carbon nanotube and graphene show high effectiveness for both electrochemical and hybrid supercapacitors. These carbon materials however, have limitations of high cost and involve highly toxic oxidants for synthesis methods [2]. The objective of this research is to produce carbon-based materials which show a porous structure with a high surface, high conductivity, suitable pore size distribution, and long-term cyclability from low-cost raw materials by simple synthesis methods for use as electrodes.

Biomass is a low-cost raw carbon material with great potential for synthesizing various carbon materials, and it can be converted into biofuels for use as alternative energy sources. A wide range of biomass are derived from all types of biological resources such as plants, animals, and microbes [3]. There are many biomasses from agricultural waste such as coconut shells, rice husks, cane bagasse, bamboo, palm shell, and durian shell in Thailand. These wastes are raw carbon materials that can be converted into biochar, which is carbon materials.

Biochar is a carbon-rich material produced from biomass by thermochemical conversion as dry carbonization, pyrolysis (gasification), and hydrothermal carbonization process. Pyrolysis is the most common method for producing biochar, this method can generate biochar by heating biomass under a limited supply of oxygen. There are two types of pyrolysis processes: slow pyrolysis and fast pyrolysis, depending on the heating rate and soaking time. The difference between the two types of processes is the yield of char and tar. Slow pyrolysis produce biochar by heating biomass at a low heating rate and long soaking time, this process gives high yield biochar at about 20 - 50%. Fast pyrolysis produce biochar at a high heating rate (above 200 °C/min) and short soaking time (less than 10 seconds), this process gives a high yield of tar but low yield biochar at about 10 - 20% [1], [3] - [4]. There are three main components of biomass as cellulose, hemicellulose, and lignin at about 40 - 60%, 20 - 40%, and 10 - 25%, respectively. In the cell walls of plants, cellulose is organized into microfibril, interrupted by hemicellulose, and surrounded by lignin matrix. Cellulose, a natural linear polymer, is the major constituent, has strong fibers. Hemicelluloses

have a random amorphous structure with little strength, while lignin is a highly cross-linked and three-dimensional structure with high strength. The pyrolysis of biomass can be divided into four individual stages with the decomposition of moisture, hemicellulose, cellulose, and lignin, respectively [5] - [7].

The applications of biochar have been studied and reviewed extensively, and are applied to agricultural (soil amendment) and environmental (inorganic pollutant removal) benefits. For example, the potentials of porous and nutrients-rich of biochar to nutritionally enrich soil and in the removal of the cationic compounds from water [8] - [11]. Moreover, most of the biochars from agricultural waste are carbon materials with a porous structure; these properties are important properties of high-performance electrode materials [12] - [18]. Among the porous biochar from agricultural waste in the study of Daosukho, S., Kongkeaw, A., and Oengeaw, U. [10] found that carbon yield percentage of durian shell biochar is about 57%, it is less than the carbon yield percentages of bamboo and palm shell biochars which are about 65%. But the durian shell biochar showed higher porosity on the surface than the other biochars. Therefore the durian shell biochar is an interesting materials to be used in high-performance electrode materials.

The objective of this research was to study the effects of pyrolysis temperature on the properties of durian shell biochar, a porous carbon material to be used in high-performance electrode materials in the next study.

Experiment

1. Manufacturing

Durian shell biomass from Uttaradit province, Thailand was chosen for this research. Durian shell biochars were produced from durian shell biomass by the pyrolysis process, according to the following steps. The biomasses were cleaned in water and dried at 100 °C for 24 hours in the oven to eliminate moisture. Then, the dried-biomasses were stored into a closed - alumina chamber which did not allow air to enter from outside, and then heated in the absence of oxygen at 500 - 900 °C with a low heating rate (10 °C/min) for 10 hours in the electric furnace.

2. Characteristics

Various instruments and techniques were chosen to study the characteristics of durian shell biochar as follows:

The percent yield (*%Yield*) is the percent ratio of a product yield and raw materials yield. It was calculated from the weight of the product as biochar divided by the weight of raw material as biomass multiplied by 100%. An electronic balance (Sartorius:

Practum224-1s) was used to weigh all the samples equation (1).

$$\%Yield = \frac{Weight\ of\ Product}{Weight\ of\ Raw\ Material} \times 100 \quad (1)$$

The bulk density (ρ) and apparent porosity (%AP) of all biochars were determined by the Archimedes immersion technique with ASTM C20 standard test methods. This technique involves placing a container of the liquid under test on the electronic balance and determining the specific gravity of samples using the plummet (Sartorius: Practum224-1s with YDK03 density kit). Both values are calculated from the dry weights (D), saturated weight (W), and suspended weight (S) of biochars. Acetone which has a density of 0.7857 g/cm^3 (ρ_0) was the chosen medium liquid for this work. The biochars were placed in acetone, sonicated in an ultrasonic bath for 3 hours, and immersed for 12 hours before weighing. The saturated and suspended weights are the weights of the biochars that were weighed in air and acetone, respectively. The formulas for these calculations are as follows equation (2) - (3):

$$\rho = \frac{D}{W - S} \times \rho_0 \quad (2)$$

$$\%AP = \frac{W - D}{W - S} \times 100 \quad (3)$$

The morphologies and pore structure were observed by scanning electron microscopy (SEM: JEOL, JSM-IT300). The cross-section areas of all biochars were coated with gold, Au, metal before examination using the signal of secondary electrons images. The elemental compositions were analyzed by energy-dispersive X-ray spectroscopy (EDX), which was used together with scanning electron microscopy. Moreover, X-ray diffractometer (XRD: Rigaku, Miniflex II) was used for the identification of crystalline phases.

Results and Discussion

1. Appearances of durian shell biomass and biochars

The appearance of durian shell biomass and biochars are shown in Figure 1. The biomasses were changed to black biochars completely and the weight loss happening occurred due to fiber decomposition of biomass through pyrolysis process.

The chemical analysis from the research of Lubis, R., Saragih, S. W., Wirjosentono, B., and Eddyanto, E. [19] showed that the fiber of durian shell biomass contains

57 - 64% cellulose, 30.7% hemicellulose, and 13.6% lignin. The decomposition of hemicellulose and cellulose occurred quickly, with the weight loss of hemicellulose happening at 220 - 315 °C and that of cellulose happening at 315 - 400 °C. Lignin was more difficult to decompose and the decomposition happened at a wide temperature range between 160 - 900 °C. The main gas products from this process were CO₂, CO, and CH₄ [5]. Therefore, the tendency of biochars to yield decreased with an increase in pyrolysis temperature (Table 1) due to the increase of the decomposition of lignin.

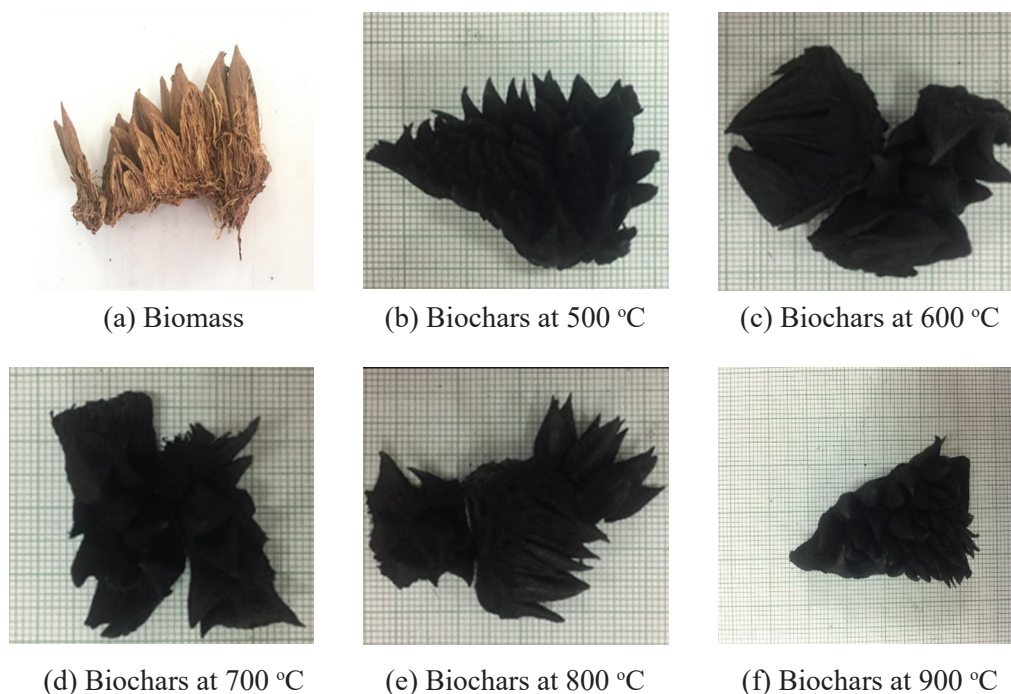


Figure 1 Appearances of durian shell biomass and biochars

Table 1 Percent yield of the biochars at different pyrolysis temperatures

Pyrolysis temperature (°C)	Yield (%)
500	46.96
600	41.43
700	37.72
800	34.44
900	28.31

2. Density and porosity

The bulk density and apparent porosity of all biochars are shown in Figure 2. The durian shell biochars have a low density of about 0.2 - 0.4 g/cm³, and the density value increased with an increase in pyrolysis temperature. It can be seen that all biochars show similar apparent porosity values of more than 70%. The durian shell biochars showed high porosity, which is one of the important properties of materials that can be developed into high-performance electrode materials.

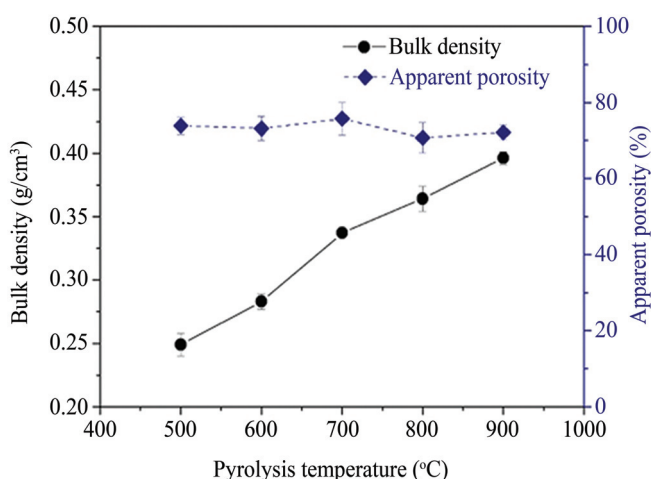


Figure 2 Bulk density and apparent porosity of the biochars at different pyrolysis temperatures

3. Morphology

The cross-section SEM images of all biochars at 1000x magnification are shown in Figure 3. Besides, the average pore size of the biochars was analyzed from these SEM images using ImageJ software. It was found that the biochars had a highly porous structure with numerous hollow cells, which were inherited from the original biomass. The average pore size increased with an increase in pyrolysis temperature (Table 2). An increase in pyrolysis temperature can also lead to the widening of pore size due to breaking down of the walls between adjacent pores [3].

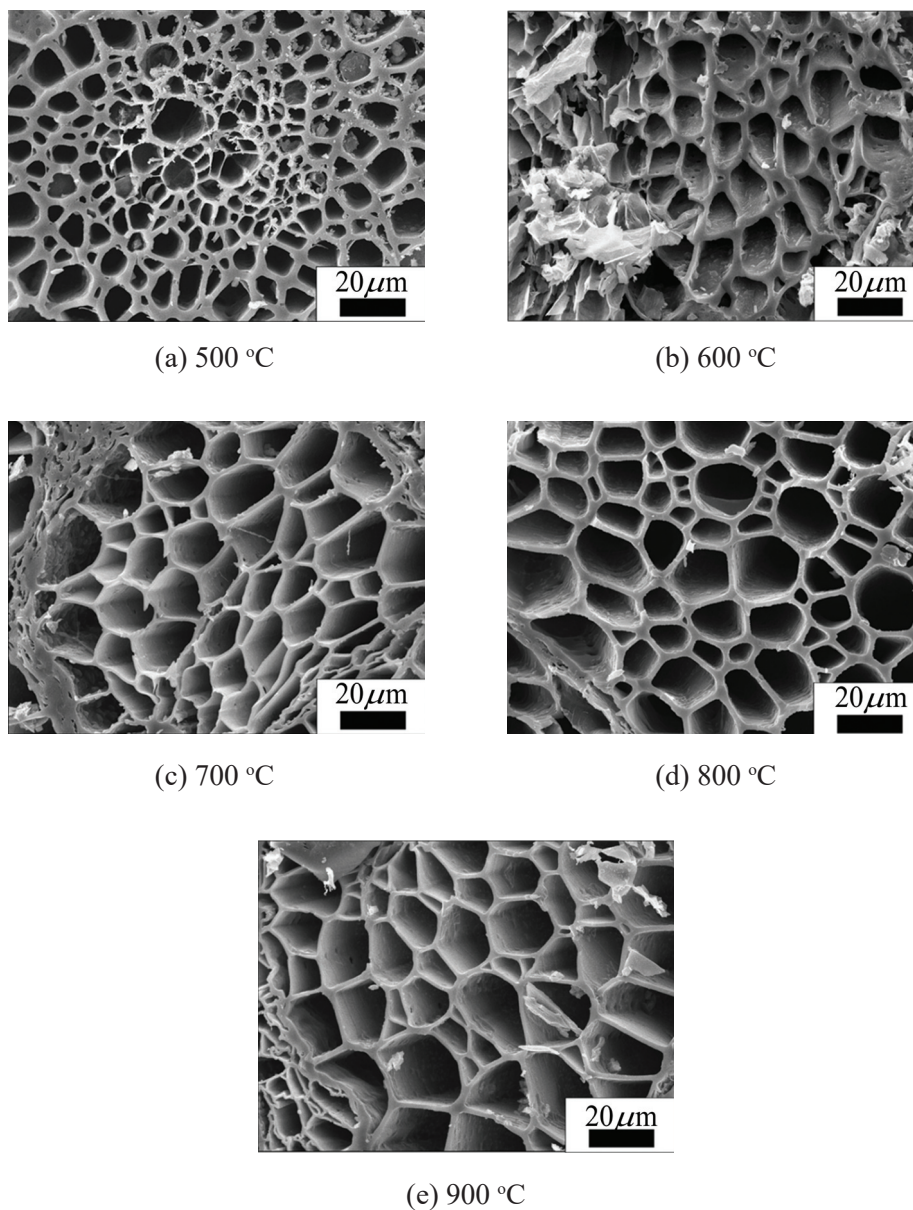
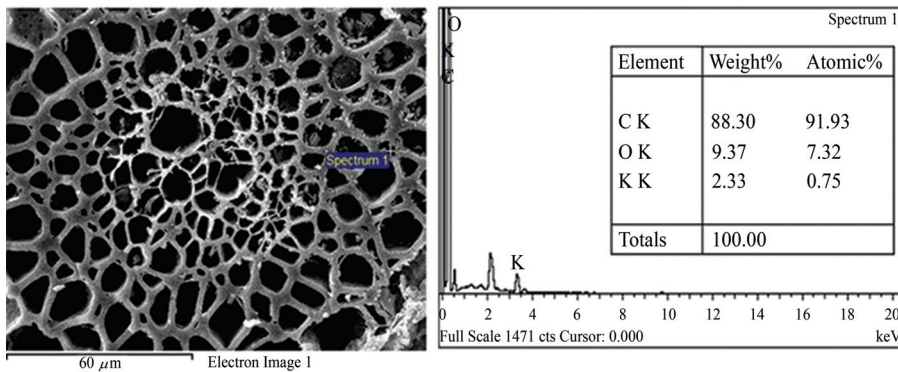


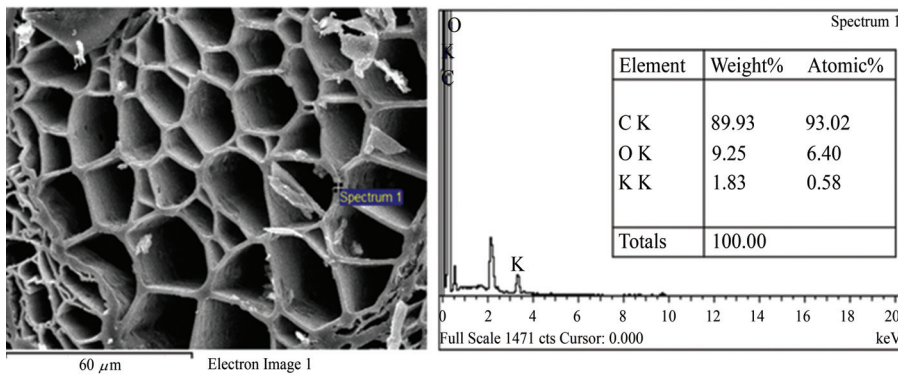
Figure 3 The cross-section SEM images of durian shell biochars at different pyrolysis temperatures at 1000x magnification

Table 2 Average pore size of the biochars at different pyrolysis temperatures

Pyrolysis temperature (°C)	Average pore size (μm)
500	7.28 ± 2.36
600	8.31 ± 3.05
700	13.02 ± 4.45
800	13.69 ± 5.00
900	15.07 ± 5.08



(a) 500 °C



(b) 900 °C

Figure 4 The morphologies at 1000x magnification, EDX spectrums and elemental compositions of the biochars which were prepared at 500 °C and 900 °C

4. Elemental compositions

Figure 4 shows the morphologies at 1000x magnification, EDX spectrums, and elemental compositions of the biochars which were prepared at 500 °C and 900 °C. It was found that the EDX spectrums of both biochars showed similar results. The main element

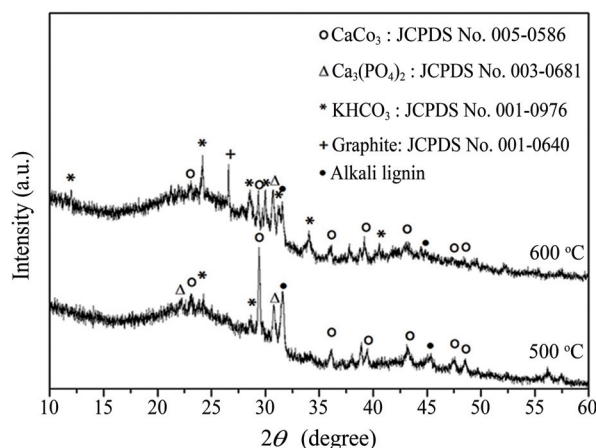
in these biochars was carbon (C) at about 88 - 90 wt%. Also, the spectrums of these biochars contained some elements, including oxygen (O) and potassium (K). These results were consistent with the other biochar conditions. A previous study found other elements in durian biochar such as phosphorus (P), magnesium (Mg), calcium (Ca), aluminum (Al), sulfur (S), Iron (Fe), Manganese (Mn) and Arsenic (As) [9]. These elements could be composed with oxygen or chlorine in the forms to oxides, carbonates, phosphates or chloride structures such as KH_2PO_4 (Archerite), CaCO_3 (Calcite), KCaCl_3 (Chlorocalcite), KHCO_3 (kalicinite), $\text{NH}_4\text{MgPO}_4 \cdot 6\text{H}_2\text{O}$ (Struvite) and KCl (Sylvite) [9] - [10]. X-ray diffraction techniques confirmed these crystalline phases of biochars in this work.

5. Crystalline phases

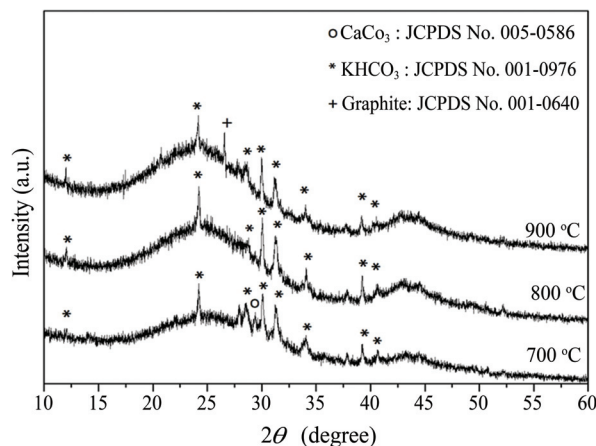
The XRD patterns of all biochars are shown in Figure 5. Broad peaks atypical at 2θ about $20 - 30^\circ$ and $40 - 50^\circ$ are observed in the XRD pattern of 500°C , 700°C and 800°C biochars conditions, which indicated the amorphous state of carbon in biochars. While, the XRD patterns of 600°C and 900°C biochars conditions indexed sharp peak of graphite crystal at $2\theta = 26.5^\circ$ (002) and broad peaks atypical at 2θ about $40 - 50^\circ$ of amorphous state so, these conditions indicated semi-crystalline state of carbon. Therefore the formation of carbon phases in biochar can occur in both amorphous and semi-crystalline phases. A review of Lin, W-J., Jiang, H., and Yu, H-Q. [3] said that this semi-crystalline structure occurred from the natural structure of biobased polymer derived from the biomass, which has mainly amorphous structure, and some local crystalline structure of highly conjugated aromatic sheet cross-linked randomly. Moreover, the biochar crystallite can increase in size and the entire structure becomes more ordered with increasing pyrolysis temperatures.

Also, the XRD patterns of 500°C and 600°C conditions (Figure 5(a)) indexed sharp peaks of many mineralogical compositions as CaCO_3 (Calcite), KHCO_3 (kalicinite) and $\text{Ca}_3(\text{PO}_4)_2$. Moreover, the sharp peak at $2\theta = 31.6^\circ$ and $2\theta = 45.4^\circ$ are indexed on XRD patterns of only these biochar conditions. These peaks correspond with alkali lignin sharp peak in the research of Ye, X-X., Luo, W., Lin, L., Zhang, Y-Q., and Liu, M-H. [20], which studied the preparation of lignin-based dye dispersant from alkali lignin of Masson pine sulfite pulping liquor. Lignin is hard to decompose due to the highly cross-linked and three-dimensional structure. The thermogravimetric analysis (TGA) curve in the research of Yao, B., Kolla, P., Koodali, R., Balaranjan, S., Shrestha, S., and Smirnova, A. [7] found that the decomposition of the original lignin starts at 350°C and at 480°C almost 80% of lignin is decomposed. The TGA curve in the research of Yang, H., Yan, R., Chen, H., Lee, D. H., and Zheng, C. [5] found that the decomposition of lignin happened at a wide temperature

range between 160 - 900 °C. The durian shell fiber consists of approximately 13.6% lignin [19]. So, the possibility of lignin decomposition is not complete at 500 °C and 600 °C.



(a) 500 °C and 600 °C



(b) 700 °C, 800 °C and 900 °C

Figure 5 The XRD patterns of the biochars at different pyrolysis temperatures

The XRD patterns of 700 - 900 °C conditions (Figure 5(b)) indexed the sharp peaks of KHCO_3 , which was the major phase. Considering the XRD patterns of all biochars, it was found that the pyrolysis temperature affects the type of phases in biochars. The CaCO_3 phase was the major phase at 500 °C, the sharp peak intensity of this phase decreased with increasing temperatures and disappeared with the heating temperature of 800 °C. The results indicated the decomposition of the CaCO_3 phase at a high temperature of biochar. The decomposition of the CaCO_3 phase can be confirmed by the TGA curve of CaCO_3 particles in the research of Babou-Kammoe, R., Hamoudi, S., Larachi, F., and

Belkacemi, K. [21]. The weight loss of CaCO_3 began to occur at the decomposition temperature of 552 °C and finished at about 740 °C, the products of this decomposition are CaO and CO_2 . The $\text{Ca}_3(\text{PO}_4)_2$ phase appeared only in XRD patterns of 500 °C and 600 °C conditions. The TGA curves of calcium phosphate phase in the research of Granados-Correa, F., Bonifacio-Martínez, J., and Serrano-Gómez, J. [22] showed the calcium phosphate was stable at temperatures below 600 °C and the phosphate ion decomposition observed at 642 and 697 °C. While the KHCO_3 phase formed at high temperature and a thermal stability higher than CaCO_3 and $\text{Ca}_3(\text{PO}_4)_2$ phases.

Conclusion

The fibers of durian shell biomass contain cellulose, hemicellulose, and lignin. All of these fibers can be decomposed to biochars, which are carbon-rich materials with high porosity, by pyrolysis process. The decomposition of hemicellulose and cellulose fibers occurred quickly at low temperatures, but lignin is hard to decompose due to its highly cross-linked structure, which could use heating temperature of more than 600 °C. The natural structure of biobased polymer derived from the biomass can be formed to both amorphous and semi-crystalline phases of carbon. While, oxygen could be composed in other elements in biomass through many forms of mineralogical compositions as CaCO_3 , KHCO_3 , and $\text{Ca}_3(\text{PO}_4)_2$. The CaCO_3 and $\text{Ca}_3(\text{PO}_4)_2$ phases can be decomposed at pyrolysis temperature lower than 700 °C, but the KHCO_3 phase is formed at high temperature and has a thermal stability higher than CaCO_3 and $\text{Ca}_3(\text{PO}_4)_2$ phases.

Acknowledgment

The authors would like to thank Phranakhon Rajabhat University for funding this research. The authors would also like to thank the Electroceramics laboratory, department of physics and materials science, Chiang Mai University, for providing the advanced instruments for fabrication in this research. Finally, the authors would like to acknowledge Asst. Prof. Dr. Sukum Eitssayeam and Ms. Katsirin Sangmanee for offering recommendations.

References

- [1] Xiu, S., Shahbazi, A., and Li, R. (2017). Characterization, Modification, and Application of Biochar for Energy Storage and Catalysis: A Review. **Trends in Renewable Energy**. Vol. 3, No. 1, pp. 86-101. DOI: 10.17737/tre.2017.3.1.0033

- [2] Jin, H., Wang, X., Gu, Z., and Polin, J. (2013). Carbon Materials from High Ash Biochar for Supercapacitor and Improvement of Capacitance with HNO₃ Surface Oxidation. **Journal of Power Sources**. Vol. 236, pp. 285-292. DOI: 10.1016/j.jpowsour.2013.02.088
- [3] Lin, W-J., Jiang, H., and Yu, H-Q. (2015). Development of Biochar-Based Functional Materials: Toward a Sustainable Platform Carbon Material. **Chemical Reviews**. Vol. 115, pp. 12251-12285. DOI: 10.1021/acs.chemrev.5b00195
- [4] Lehmann, J., Amonette, J. E., and Roberts, K. (2010). Role of Biochar in Mitigation of Climate Change. **Handbook of Climate Change and Agroecosystems**. pp. 343-363. DOI: 10.1142/9781848166561_0018
- [5] Yang, H., Yan, R., Chen, H., Lee, D. H., and Zheng, C. (2007). Characteristics of Hemicellulose, Cellulose and Lignin Pyrolysis. **Fuel**. Vol. 86, pp. 1781-1788. DOI: 10.1016/j.fuel.2006.12.013
- [6] Penjumras, P., Abdul Rahman, R. B., Talib, R. A., and Abdand, K. (2014). Extraction and Characterization of Cellulose from Durian Rind. **Agriculture and Agricultural Science Procedia**. Vol. 2, pp. 237-243. DOI: 10.1016/j.aaspro.2014.11.034
- [7] Yao, B., Kolla, P., Koodali, R., Balaranjan, S., Shrestha, S., and Smirnova, A. (2017). Laccase-Natural Mediator Systems for “Green” Synthesis of Phenolic Monomers from Alkali Lignin. **Sustainable Energy Fuels**. Vol. 1, Issue 7, pp. 1573-1579. DOI: 10.1039/C7SE00209B
- [8] Prakongkep, N., Gilkes, R. J., and Wiriyaakitnateekul, W. (2015). Forms and Solubility of Plant Nutrient Elements in Tropical Plant Waste Biochars. **Journal of Plant Nutrition and Soil Science**. Vol. 178, Issue 5, pp. 732-740. DOI: 10.1002/jpln.201500001
- [9] Prakongkep, N., Gilkes, R. J., and Wiriyaakitnateekul, W. (2014). Agronomic Benefits of Durian Shell Biochar. **Journal of Metals, Materials and Minerals**. Vol. 24, No. 1, pp. 7-11. DOI: 10.14456/jmmm.2014.2
- [10] Daosukho, S., Kongkeaw, A., and Oengeaw, U. (2012). The Development of Durian Shell Biochar as a Nutrition Enrichment Medium for Agricultural Purpose: Part 1 Chemical and Physical Characterization. **Bulletin of Applied Sciences**. Vol. 1, No. 1, pp. 133-141
- [11] Tsai, W-T., Hsu, C-H., and Lin, Y-Q. (2019). Highly Porous and Nutrients-Rich Biochar Derived from Dairy Cattle Manure and Its Potential for Removal of Cationic Compound from Water. **Agriculture**. Vol. 9, pp. 114-123
- [12] Qie, L., Chen, W., Xu, H., Xiong, X., Jiang, Y., Zou, F., Hu, X., Xin, Y., Zhang, Z., and Huang, Y. (2013). Synthesis of Functionalized 3D Hierarchical Porous Carbon for High-Performance Supercapacitors. **Energy and Environmental Science**. Vol. 6, Issue 8, pp. 2497-2504. DOI: 10.1039/C3EE41638K
- [13] Zhang, K., Shang, Z., Wu, S., Wang, J., Sheng, W., Shen, X., and Zhu, M. (2017). Commercialized Benzoxazine Resin-Derived Porous Carbon as high Performance Electrode Materials for Supercapacitor. **Journal of Inorganic and Organometallic Polymers and Materials**. Vol. 27, Issue 5, pp. 1423-1429. DOI: 10.1007/s10904-017-0596-7

- [14] Niu, J., Shao, R., Liang, J., Dou, M., Li, Z., Huang, Y., and Wang, F. (2017). Biomass-Derived Mesopore-Dominant Porous Carbons with Large Specific Surface Area and High Defect Density as High Performance Electrode Materials for Li-ion Batteries and Supercapacitors. **Nano Energy**. Vol. 36, pp. 322-330. DOI: 10.1016/j.nanoen.2017.04.042
- [15] Li, J., Gao, Y., Han, K., Qi, J., Li, M., and Teng, Z. (2019). High Performance Hierarchical Porous Carbon Derived from Distinctive Plant Tissue for Supercapacitor. **Scientific Reports**. Vol. 9, p. 17270. DOI: 10.1038/s41598-019-53869-w
- [16] Zhu, Y., Fang, T., Hua, J., Qiu, S., Chu, H., Zou, Y., Xiang, C., Huang, P., Zhang, K., Lin, X., Yan, E., Zhang, H., Xu, F., Sun, L., and Zeng, J-L. (2019). Biomass-Derived Porous Carbon Prepared from Egg White for High-performance Supercapacitor Electrode Materials. **Chemistry Select**. Vol. 4, Issue 24, pp. 7358-7365. DOI: 10.1002/slct.201901632
- [17] Phiri, J., Dou, J., Vuorinen, T., Gane, P. A. C., and Maloney, T. C. (2019). Highly Porous Willow Wood-Derived Activated Carbon for High-Performance Supercapacitor Electrodes. **ACS Omega**. Vol. 4, pp. 18108-18117. DOI: 10.1021/acsomega.9b01977
- [18] Wei, M.-M., Li, W.-P., Weng, J., Liu, Y.-Q., Li, S.-R., Ye, Y.-Y., Wang, M., and Wang, D. (2019). Mesopore-Dominant Porous Carbon Derived from Bio-Tars as an Electrode Material for High-Performance Supercapacitors. **Journal of Saudi Chemical Society**. Vol. 23, Issue 7, pp. 958-966. DOI: 10.1016/j.jscs.2019.04.002
- [19] Lubis, R., Saragih, S W., Wirjosentono, B., and Eddyanto, E. (2018). Characterization of Durian Rinds Fiber (*Durio zubinthinus, murr*) from North Sumatera. **AIP Conference Proceedings**. Vol. 2049, Issue 1, pp. 020069. DOI: 10.1063/1.5082474
- [20] Ye, X-X., Luo, W., Lin, L., Zhang, Y-Q., and Liu, M-H. (2017). Quaternized Lignin-Based Dye Dispersant: Characterization and Performance Research. **Journal of Dispersion Science and Technology**. Vol. 38, Issue 6, pp. 852-859. DOI: 10.1080/01932691.2016.1207545
- [21] Babou-Kammoe, R., Hamoudi, S., Larachi, F., and Belkacemi, K. (2012). Synthesis of CaCo₃ Nanoparticles by Controlled Precipitation of Saturated Carbonate and Calcium Nitrate Aqueous Solutions. **The Canadian Journal of Chemical Engineering**. Vol. 90, Issue 1, pp. 26-33. DOI: 10.1002/cjce.20673
- [22] Granados-Correa, F., Bonifacio-Martínez, J., and Serrano-Gómez, J. (2010). Synthesis and Characterization of Calcium Phosphate and Its Relation to Cr (VI) Adsorption Properties. **Revista internacional de Contaminación Ambiental**. Vol. 26, No. 2, pp. 129-134